A Microwave Communication Link With Self-Heterodyne Direct Down Conversion and System Predistortion

Jin Park, *Student Member, IEEE*, Yuanxun Wang, *Member, IEEE*, and Tatsuo Itoh, *Fellow, IEEE*

***Abstract*—A novel design of a microwave communications link operating at 5.8 GHz is presented based on self-heterodyne direct downconversion (SHDDC) and system predistortion. Utilizing the SHDDC scheme eliminates the need of any local oscillators at the receive ends and minimizes spectrum usage; however, the transmitter power efficiency is low, and there exist high mixer intermodulation levels in the receiver. To overcome these drawbacks, a system predistortion approach is proposed. A two-tone measurement is performed to validate the idea. It shows 12.67 dBc of overall improvement in the signal-to-intermodulation ratio by applying a fourth-order predistortion technique. Further, successful transmission of a digitally modulated signal is also demonstrated.**

***Index Terms*—Direct downconversion, predistortion, self-heterodyne.**

I. INTRODUCTION

CURRENT microwave data transmission predominately utilizes the super-heterodyne scheme, in which a devoted local oscillator (LO) is required at the receiver end to pump the mixer and downconvert the RF signal. The LO power is usually much greater than the RF signal power, thus minimizing the distortion caused by the self-product terms of the RF signal in the mixer output. One alternative to the super-heterodyne method is the self-heterodyne scheme [1]. In this scheme, the transmitter sends out the local carrier as well as the modulated RF signal. The received signal is demodulated by passing it through a self-mixer. The self-heterodyne scheme significantly reduces the circuit complexity at the receiver, eliminating the need to supply a LO circuit and the related carrier recovery circuit. Such a system is especially suited for broadcasting applications where the number of receive terminals is large and the size and complexity of each terminal are limited. This has been applied in millimeter-wave communication systems [1] where the implementation of an LO with low phase noise is technically difficult.

One drawback of the self-heterodyne system is that extra intermodulation distortion is introduced. Due to the limited carrier power received, the self-product terms of RF signal can no longer be neglected when compared to the IF output. One has to compromise between the transmitter power efficiency and the intermodulation level of the mixer output. One approach to overcome this problem is to carefully choose an IF frequency which is much higher than the signal bandwidth, allowing the intermodulation term to be filtered out. However, this approach has low spectrum efficiency and requires extra IF demodulators.

Manuscript received April 5, 2002; revised August 23, 2002.

The authors are with the Department of Electrical Engineering, University of California, Los Angeles, CA 90095 USA (e-mail: itoh@ee.ucla.edu).

Digital Object Identifier 10.1109/TMTT.2002.805134

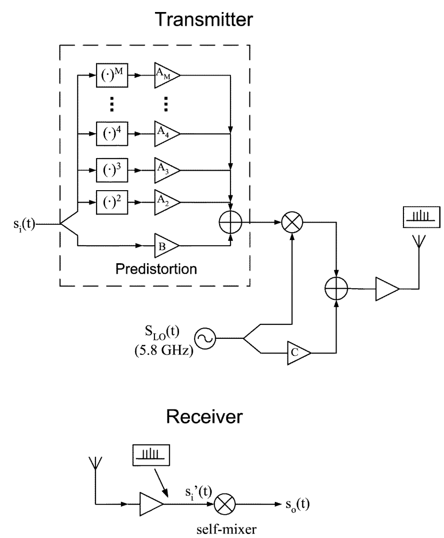

Fig. 1. Transmitter and receiver block diagrams.

In this paper, a self-heterodyne direct down conversion (SHDDC) microwave communication link is proposed with the system predistortion technique. The essential idea of system predistortion is to predistort the baseband signal in the transmitter to compensate the intermodulation at the receiver mixer output caused by the proximity of the LO and RF power levels. Hence, the simplicity of the self-heterodyne scheme and the high spectrum efficiency of the direct down conversion receiver are both maintained.

This paper is organized as follows. In Section II, the system predistortion concepts and the basic operation principles are introduced based on nonlinear power series analysis. In Section III, a testbed with a 5.8-GHz carrier frequency is set up, measured results for a two-tone signal are found to validate the proposed idea, and successful transmission of digital data modulated in 4-ary amplitude-shift keying (ASK) format [2] is demonstrated.

II. SHDDC SYSTEM OVERVIEW

A. Nonlinear System Analysis

Theoretical validity of the SHDDC system is accomplished by applying power series nonlinear circuit analysis [3]. Fig. 1 shows the block diagram of the communications system. For a general nonlinear circuit, the excitation can be expressed as

$$v_i(t) = 1/2 \sum_{\substack{q=-Q \\ q\neq 0}}^{Q} V_q e^{jw_q t}. \tag{1}$$

The resulting power series expression for the circuit output is

$$v_0(t) = \sum_{n=1}^{N} a_n \left[\frac{1}{2} \sum_{q=-Q}^{Q} V_q H(w_q) e^{jw_q t} \right]^n. \tag{2}$$

In (1) and (2), $V_{-q} = V_q^*$, $w_{-q} = -w_q$, and $H(w_{-q}) = H^*(w_q)$. Assuming for simplicity a memoryless, nondispersive propagation channel such that $H(w_q) = 1$ for all q, the output expression simplifies to

$$v_0(t) = \sum_{n=1}^{N} a_n [v_i(t)]^n. \tag{3}$$

Letting the system excitation $s_i(t) = v_i(t)$ and ignoring the amplifiers before the transmit antenna and after the receive antenna, refer to Fig. 1 to obtain the expression at the input of the self-mixer, which is expressed as follows:

$$\begin{aligned} s_i'(t) = \left[A_2 s_i^2(t) + A_3 s_i^3(t) + \cdots + A_M s_i^M(t) + B s_i(t) \right] \\ \times s_{\mathrm{LO}}(t) + C s_{\mathrm{LO}}(t). \end{aligned} \tag{4}$$

Utilizing the transfer function assumption of before, the resulting power series expression for the final output of the system is

$$s_0(t) = \sum_{n=1}^{N} a_n \left[s_i'(t) \right]^n. \tag{5}$$

Expanding (5) with second-order distortion $(M = 2)$ and $N = 2$ yields

$$\begin{aligned} s_o(t) =& s_{\mathrm{LO}}(t) \times \left[a_1 A_2 s_i^2(t) + a_1 B s_i(t) + a_1 C \right] + s_{\mathrm{LO}}^2(t) \\ &\times \left[a_2 A_2^2 s_i^4(t) + a_2 2 A_2 B s_i^3(t) \right. \\ &+ a_2 B^2 s_i^2(t) + a_2 2 A_2 C s_i^2(t) \\ &\left. + a_2 2 B C s_i(t) + a_2 C^2 \right]. \end{aligned} \tag{6}$$

The final baseband components are embedded in the $s_{\mathrm{LO}}^2(t)$ term of (6). One now recognizes that cancellation of second-order terms occurs if

$$2A_2 C = -B^2. \tag{7}$$

The third- and fourth-order terms cannot be cancelled merely with second-order distortion. Expanding (5), one realizes that higher order distortion can be used to decrease these higher order terms: third-order predistortion to cancel third-order terms, fourth-order predistortion to cancel fourth-order terms, and so on. In general, to reduce Nth-order terms of the baseband signal $s_i(t)$, one needs Nth-order predistortion. Note that all higher order terms cannot be cancelled simultaneously. The predistortion coefficients can only be adjusted to minimize the aggregate distortion of the system. One can also recognize that the final baseband components are contained only within even powers of $s_{LO}(t)$ or only for even n in (5). Expanding (5) with third-order distortion $(M = 3)$, $N = 4$, and omitting nonbaseband components yields

$$\begin{aligned} s_0(t) = & \left[s_i^2(t) \left[a_2 \left(B^2 + 2A_2 C \right) + a_4 \left(6B^2 C^2 + 4A_2 C^3 \right) \right] \right. \\ & + s_i^3(t) \left[a_2 (2A_2 B + 2A_3 C) \right. \\ & \left. \left. + a_4 \left(4B^3 C + 12 A_2 B C^2 + 4 A_3 C^3 \right) \right] \right]. \end{aligned} \tag{8}$$

From (8), it is apparent that reduction of the second- and third-order terms can be accomplished by choosing the appropriate values for the second- and third-order predistortion coefficients (A_2, A_3). Further expansions of (5) for various M and N show that suitable selection of predistortion coefficients $(A_2, A_3, \ldots, A_M)$ minimizes the effect of the higher order baseband terms.

Note that in (6), there arises a dc component to the signal, which is represented by the $a_2 C^2$ term. This dc offset is caused by the use of direct down conversion and is not desirable. Referring to Fig. 1, this dc term is proportional to the square of the LO amplification factor C. Recalling that the use of the predistortion technique allows for lower required LO power, the amount of dc offset is reduced as compared to conventional direct conversion receivers. For certain cases with stringent dc offset requirement, adaptive dc offset cancellation circuits can be employed to overcome the problem.

The preceding development validates the system predistortion concept theoretically using simplified nonlinear power series analysis.

B. System Operation

Predistortion of the original baseband signal is performed via Agilent's HP34811A Benchlink software application. This software interfaces conveniently with the HP33120A arbitrary waveform generator used during measurement. In general, the predistortion coefficients can be complex. For this paper, scalar predistortion is examined to verify the validity of the system concept. Further, only $A_2, A_3, \ldots$, and A_M are varied during measurement; B is held constant and made equal to one. The case in which $B = 1$ and $A_2 = A_3 = \cdots = A_M = 0$ represents the reference case in which there is no predistortion. Note that C is constant and positive during operation. Also assume that the power series coefficients a_n are positive. From (7), one realizes that to achieve cancellation using second order predistortion, scalar manipulation of A_2 requires A_2 to have a negative value. From (8), it is again necessary to have A_2 less than zero to minimize the second order baseband term. For the third-order baseband term in (8), it becomes evident that the third-order predistortion coefficient (A_3) can be positive or negative.

The baseband signal is upconverted via analog amplitude modulation. Sufficient LO leakage exists to produce the desired carrier in the self-heterodyne scheme. After power amplification, the RF signal is transmitted and received using quasi-Yagi antennas [4]. These antennas are characterized by endfire radiation, broad operating bandwidth, and moderate gain.

Direct downconversion is achieved with an active self-mixer, which is shown in Fig. 2. Desired downconversion is accomplished by adding open stubs at the self-mixer's output that effectively look like short circuits at the first two harmonics of the carrier frequency, namely 5.8 and 11.6 GHz. This requires one stub to be $\lambda/4$ long (5.8 GHz short) and the other to be $\lambda/8$

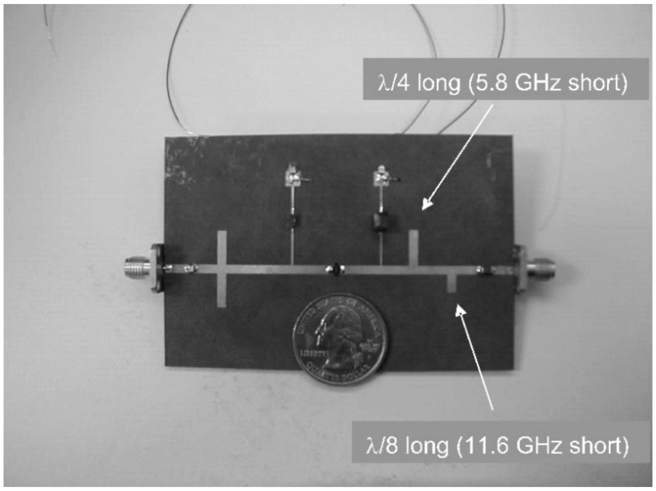

Fig. 2. Self-mixer circuit.

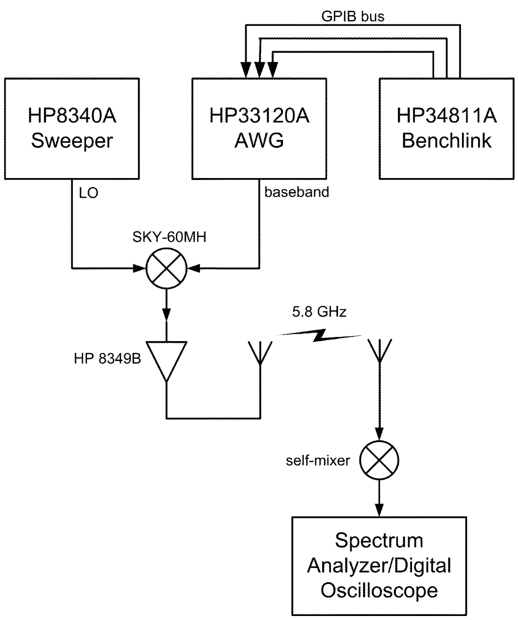

Fig. 3. Predistortion system measurement setup.

in length (11.6-GHz short). A circuit optimizer (Agilent's Advanced Design System 2001) is used to find an acceptable input matching circuit. The circuit uses NEC's NE76038 as the active device, and fabrication is done on RT/Duroid 5880 with a dielectric constant of 2.33 and a substrate thickness of 31 mL.

III. Measurement Setup and Results

A. Experimental Setup

Fig. 3 shows the measurement setup for the predistortion system. Agilent's HP33120A arbitrary waveform generator and HP34811A Benchlink software package are consolidated to generate the desired baseband waveform. Agilent's HP8340A synthesized sweeper generates the 5.8-GHz oscillator to pump Mini-Circuits' SKY-60 MH four-diode bridge mixer. This upconverter yields sufficient LO leakage to generate the local carrier required with the self-heterodyne scheme. Before wireless transmission, Agilent's HP8349B microwave amplifier offering high output power $(\sim 20\ \mathrm{dBm})$ is used to boost the RF signal. The transmission distance between the transmit and receive antennas is about 8 cm, which is greater than the far-field distance associated with the antennas being used. Because the microwave amplifier provides high output power and the transmission distance is relatively short, a gain block preceding the receiver self-mixer is not necessary.

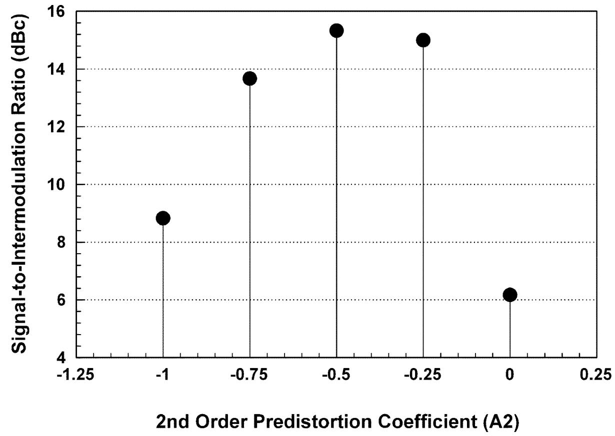

Fig. 4. SIMR ratio for various values of A_2.

B. Two-Tone Measurement

In this section, second-, third-, and fourth-order predistortion is executed experimentally. The effect of applying various combinations of predistortion coefficients (A_2, A_3, A_4) to a two-tone signal with 2- and 3-MHz components is examined, thus validating the system predistortion idea. This kind of signal represents a simplified form of a realistic digital signal, extracting only two of the many frequency components present in a digital signal. It is important in the SHDDC scheme to consider the carrier power relative to the RF power. For acceptable transmission efficiency, the carrier power should approximately equal the total RF power. Measured results show carrier power of 1.00 dBm and RF power of −6.33 dBm just preceding the receiver self-mixer stage.

For second-order predistortion, only the coefficient A_2 is varied. As mentioned in Section II-B, A_2 should have a negative value. Fig. 4 shows the signal-to-intermodulation ratio (SIMR) at the system output for various values of A_2. SIMR is defined as the power ratio of the final baseband signal (2 or 3 MHz) to the highest intermodulation tone. The highest intermodulation invariably occurs at 1 MHz. The normalized parameter in the measurement is the final signal power level at the two original tones (2 and 3 MHz). This power level is determined to be −36.83 dBm. The SIMR for the reference case $(A_2 = A_3 = A_4 = 0)$ is 6.17 dBc. From Fig. 4, using $A_2 = -0.50$ yields the best SIMR result. This optimized SIMR is 15.33 dBc, which is 9.16 dB higher than the reference SIMR. Thus, there is 9.16 dB intermodulation reduction when applying second-order predistortion.

When employing third-order predistortion, it is now important to note that the third-order predistortion coefficient (A_3) can be positive or negative. The reason for this is explained earlier. Five discrete values for A_2 and nine discrete values for A_3 are considered during measurement. This leads to 45 possible combinations of (A_2, A_3) pairs. Because a brute force measurement is executed, testing this many combinations becomes tedious. This becomes even more evident when considering fourth-order predistortion, with which there would be 405

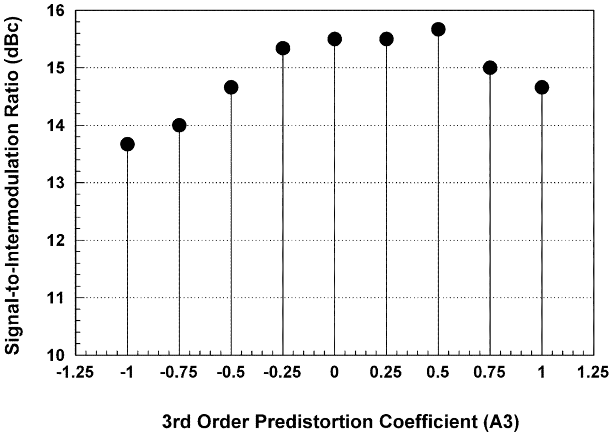

Fig. 5. SIMR ratio for various values of A_3 with optimized A_2.

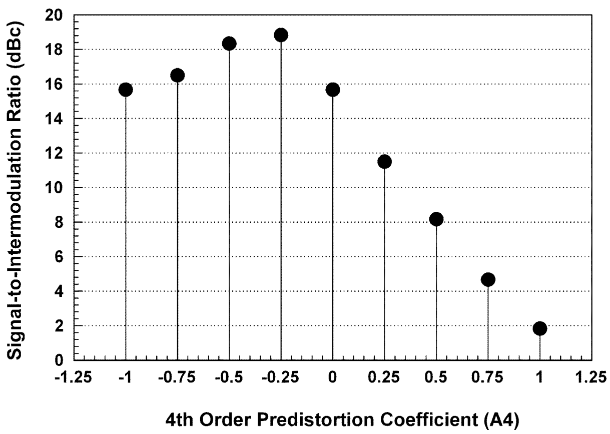

Fig. 6. SIMR ratio for various values of A_4 with optimized A_2 and A_3.

combinations. To remedy this daunting task, the following procedure is used to prevent making measurements for each possible predistorted waveform. First, second-order predistortion is executed and an optimum value for the corresponding predistortion coefficient (A_2) is determined. Next, this optimum A_2 value is used to carry out the third-order predistortion measurements; a corresponding optimum third-order predistortion coefficient (A_3) value can be determined. Finally, the optimum A_2 and A_3 values are used to execute fourth-order predistortion; a corresponding optimum fourth-order predistortion coefficient (A_4) value can be determined. This process results in making measurements for 23 waveforms.

Utilizing the above procedure, Fig. 5 shows the SIMR at the system output for various values of A_3 using the optimized A_2 value. Fig. 6 shows the SIMR at the system output for various A_4 values using optimum values for A_2 and A_3. For third-order predistortion, refer to Fig. 5 to observe that an optimum SIMR equal to 15.67 dBc occurs with $A_3 = +0.50$. For fourth-order predistortion, Fig. 6 reveals an optimum SIMR of 18.83 dBc occurs with $A_4 = -0.25$. These results for various orders of predistortion are tabulated in Table I. Note the slight improvement in SIMR from second- to third-order predistortion of 0.33 dB, and the significant improvement from third- to fourth-order predistortion of 3.16 dB. This difference in the amount of SIMR improvement from second to third-order predistortion versus third- to fourth-order predistortion can be explained by reevaluating the definition of SIMR. For simplicity, SIMR is defined as the power ratio between the baseband signal, which has tones at 2 and 3 MHz, to the highest intermodulation tone, which invariably occurs at 1 MHz. This definition reflects a few particular terms rather than the overall intermodulation performance. Therefore, employing different orders of predistortion may effect individual intermodulation terms differently. Extending this analysis to higher orders, SIMR performance would be expected to improve similarly.

TABLE I
OPTIMIZED PREDISTORTION COEFFICIENTS AND SIMR VALUES

Coefficient Order	Coefficient Variable	Optimized Value	SIMR (dBc)
Reference	N/A	N/A	6.17
2nd	A_2	-0.50	15.33
3rd	A_3	+0.50	15.67
4th	A_4	-0.25	18.83

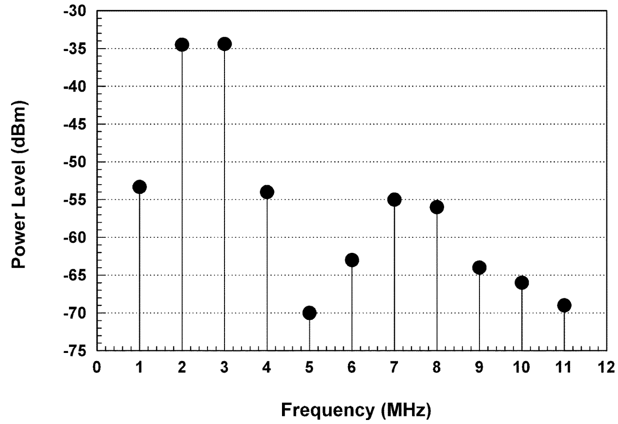

Fig. 7. Baseband power spectrum at system output using optimized predistortion coefficients.

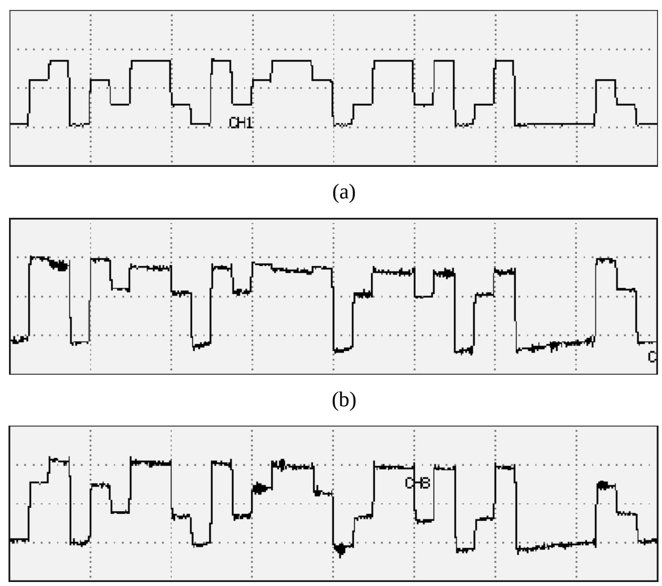

(a)

(b)

(c)

Fig. 8. (a) Original 2-Mb/s 4-ary ASK signal. (b) Demodulated signal without predistortion. (c) Demodulated signal with predistortion.

Fig. 7 shows the corresponding output baseband spectrum of the system using the optimized values for A_2, A_3, and A_4. The largest intermodulation components are of second order, with the 1-MHz term contributing the most intermodulation. One can further suppress higher frequency components with implementation of a low-pass filter.

C. 4-Ary ASK Measurement

After validating the system predistortion idea via two-tone measurement analysis, successful recovery of a digital signal should be demonstrated. Digital data with a 2-Mb/s data rate modulated in 4-ary ASK format is considered for this measurement. Fig. 8 shows the original undistorted digital signal, the demodulated signal without predistortion, and the demodulated signal with predistortion. From Fig. 8(b), one can observe the errors in the signal recovery without using predistortion. Conversely, Fig. 8(c) shows successful demodulation of the original digital signal utilizing predistortion.

IV. Conclusion

A novel design of a microwave communications link operating at 5.8 GHz using SHDDC and system predistortion is proposed. Implementation of an SHDDC scheme removes the necessity of LOs in the receiver, thus considerably simplifying the receiver circuit complexity. This is desirable for applications with many receiving terminals with restrictions on circuit size and complexity. Because SHDDC inherently has high intermodulation levels, system predistortion is proposed to lessen such effects. To validate the proposed system concept, two-tone measurement is executed with second-, third-, and fourth-order predistortion. As the order of predistortion increases, the SIMR performance improves. Finally, successful demodulation of a 4-ary ASK signal is demonstrated. Due to the brute force nature of the current measurement setup, ACPR analysis of a CDMA signal cannot be examined experimentally until a real-time adaptive system is developed. Future work will also include the development of in-phase and quadrature (I/Q) modulation schemes and the employment of complex predistortion coefficients to compensate for channel dispersion effects.

Acknowledgment

The authors wish to thank S.-S. Jeon, University of California at Los Angeles (UCLA), and R. Miyamoto, UCLA for their assistance.

References

[1] Y. Shoji, H. Ogawa, H. Nakano, Y. Hirachi, S. Nishi, and Y. Shimomichi, "Development of millimeter-wave video transmission system II—Development of millimeter-wave wireless module for remote self-heterodyne scheme," in *Proc. TSMMW*, Japan, Mar. 2000, pp. 193–196.

[2] B. P. Lathi, *Modern Digital and Analog Communication Systems*. New York: Oxford Univ. Press, 1998.

[3] S. A. Mass, *Nonlinear Microwave Circuits*. Norwood, MA: Artech House, 1988.

[4] Y. Qian, W. R. Deal, N. Kaneda, and T. Itoh, "A uniplanar quasi-Yagi antenna with wide bandwidth and low mutual coupling characteristics," in *IEEE AP-S Int. Symp. Dig.*, vol. 2, Orlando, FL, 1999, pp. 924–927.

Jin Park (S'00) was born in Seoul, Korea, in 1978. He received the B.S. degree in electrical engineering from the University of Illinois at Urbana-Champaign (UIUC), in 2000, and the M.S. degree in electrical engineering from the University of California at Los Angeles (UCLA), in 2002.

He was a Summer Intern for Triquint Semiconductor in 1999 and Motorola Inc., in 2000. As a Graduate Student Researcher at UCLA, his research interests included microwave circuits and microwave system analysis.

Mr. Park is a member of Eta Kappa Nu and Tau Beta Pi, serving as an officer in both organizations while an undergraduate student at UIUC.

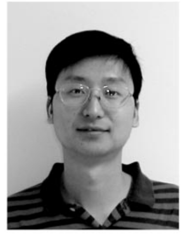

Yuanxun Wang (S'96–M'99) was born in Hubei, China, in 1973. He received the B.S. degree in electrical engineering from the University of Science and Technology of China (USTC), Hefei, China, in 1993, and the M.S. and Ph.D. degrees in electrical engineering from The University of Texas at Austin, in 1996 and 1999, respectively.

From 1995 to 1999, he was a Research Assistant with the Department of Electrical and Computer Engineering, The University of Texas at Austin. Since 1999, he has been with the Department of Electrical Engineering, University of California at Los Angeles (UCLA), where he is currently an Assistant Professor. His research interests concern the enabling technology for RF and microwave front-ends in wireless communication and radar systems, as well as the numerical modeling, simulation, and feature-extraction techniques for microwave circuits, antennas, and EM scattering. He has authored or coauthored over 60 refereed journal and conference papers.

Tatsuo Itoh (S'69–M'69–SM'74–F'82) received the Ph.D. degree in electrical engineering from the University of Illinois at Urbana-Champaign, in 1969.

From September 1966 to April 1976, he was with the Electrical Engineering Department, University of Illinois at Urbana-Champaign. From April 1976 to August 1977, he was a Senior Research Engineer with the Radio Physics Laboratory, SRI International, Menlo Park, CA. From August 1977 to June 1978, he was an Associate Professor at the University of Kentucky, Lexington. In July 1978, he joined the faculty at The University of Texas at Austin, where he became a Professor of electrical engineering in 1981 and Director of the Electrical Engineering Research Laboratory in 1984. During the summer of 1979, he was a Guest Researcher at AEG-Telefunken, Ulm, Germany. In September 1983, he was selected to hold the Hayden Head Centennial Professorship of Engineering at The University of Texas at Austin. In September 1984, he was appointed Associate Chairman for Research and Planning of the Electrical and Computer Engineering Department, The University of Texas at Austin. In January 1991, he joined the University of California at Los Angeles (UCLA), as Professor of electrical engineering and Holder of the TRW Endowed Chair in Microwave and Millimeter Wave Electronics. He was an Honorary Visiting Professor at the Nanjing Institute of Technology, Nanjing, China, and at the Japan Defense Academy. In April 1994, he became an Adjunct Research Officer for the Communications Research Laboratory, Ministry of Post and Telecommunication, Japan. He currently holds a Visiting Professorship at The University of Leeds, Leeds, U.K., and is an External Examiner of the Graduate Program of the City University of Hong Kong. He has authored or coauthored 274 journal publications, 540 refereed conference presentations, and 30 books/book chapters in the area of microwaves, millimeter-waves, antennas and numerical electromagnetics. He has generated 49 Ph.D. students.

Dr. Itoh is a member of the Institute of Electronics and Communication Engineers of Japan and Commissions B and D of USNC/URSI. He became an Honorary Life Member of the IEEE Microwave Theory and Techniques Society (IEEE MTT-S) in 1994. He was the editor-in-chief of the IEEE Transactions on Microwave Theory and Techniques (1983–1985) and the IEEE Microwave and Guided Wave Letters (1991–1994). He serves on the Administrative Committee of the IEEE MTT-S. He was vice president of the IEEE MTT-S in 1989 and president in 1990. He was the chairman of USNC/URSI Commission D (1988–1990), and Chairman of Commission D of the International URSI (1993–1996). He is the chair of the Long Range Planning Committee of URSI. He serves on advisory boards and committees of a number of organizations. He has been the recipient of a number of awards, including the 1998 Shida Award presented by the Japanese Ministry of Post and Telecommunications, the 1998 Japan Microwave Prize, the 2000 IEEE Third Millennium Medal, and the 2000 IEEE MTT-S Distinguished Educator Award.